Journal of Histochemistry & Cytochemistry 60(3) 205–218

DOI: 10.1369/0022155411435705
http://jhc.sagepub.com
SAGE

Cellular Localization and Biochemical Analysis of Mammalian CDC50A, a Glycosylated β-subunit for P4 ATPases

Dineke E. Folmer, Kam S. Mok, Sebastiaan W. de Wee, Suzanne Duijst, Johan K. Hiralall, Jurgen Seppen, Ronald P. J. Oude Elferink, and Coen C. Paulusma
Tytgat Institute for Liver and Intestinal Research, Academic Medical Center, Amsterdam, Netherlands

Summary

CDC50 proteins are β-subunits for P4 ATPases, which upon heterodimerization form a functional phospholipid translocation complex. Emerging evidence in mouse models and men links mutations in P4 ATPase genes with human disease. This study analyzed the tissue distribution and cellular localization of CDC50A, the most abundant and ubiquitously expressed CDC50 homologue in the mouse. The authors have raised antibodies that detect mouse and human CDC50A and studied CDC50A localization and glycosylation status in mouse liver cells. CDC50A is a terminal-glycosylated glycoprotein and is expressed in hepatocytes and liver sinusoidal endothelial cells, where it resides in detergent-resistant membranes. In pancreas and stomach, CDC50A localized to secretory vesicles, whereas in the kidney, CDC50A localized to the apical region of proximal convoluted tubules of the cortex. In WIF-B9 cells, CDC50A partially costains with the trans-Golgi network. Data suggest that CDC50A is present as a fully glycosylated protein in vivo, which presumes interaction with distinct P4 ATPases. (J Histochem Cytochem 60:205-218, 2012)

Keywords

β-subunit, CDC50, cholestasis, membrane, P4 ATPase, phospholipid, vesicular transport

P4 ATPases are a subfamily of P-type ATPases implicated in the transport of phospholipids from the exoplasmic to the cytosolic leaflet of biological membranes (Halleck et al. 1999; Holthuis and Levine 2005; Paulusma and Oude Elferink 2005). P4 ATPase transcripts, including alternative splice variants, are ubiquitously expressed, with most P4 ATPases in various parts of the central nervous system; exception is ATP8B3, which is almost exclusively expressed in the testis (Halleck et al. 1999; Wang et al. 2004; reviewed in Paulusma and Oude Elferink 2005; and see Allen Brain Atlas Resources at http://www.brain-map.org).

Deficiency of the mammalian P4 ATPase ATP8B1 causes progressive familial intrahepatic cholestasis type I and benign recurrent intrahepatic cholestasis type I, characterized by a chronic and a periodic cholestasis, respectively (Paulusma et al. 2010; van der Woerd et al. 2010). Besides ATP8B1, the mammalian P4 ATPase family includes 13 members, (14 in the mouse), which are poorly studied. Inactivation of some murine P4 ATPases suggests roles in fertility-related disorders, insulin resistance, and obesity (Folmer et al. 2009). Recently, ATP11C-deficient mice have been described, which display B-cell lymphopenia and intrahepatic cholestasis (Siggs et al. 2011a; Siggs et al. 2011b; Yabas et al. 2011). Studies in *Saccharomyces cerevisiae*, *Arabidopsis thaliana*, and *Caenorhabditis elegans* have indicated that P4 ATPases are important determinants

Received for publication September 12, 2011; accepted December 9, 2011.

Supplementary material for this article is available on the *Journal of Histochemistry & Cytochemistry* Web site at http://jhc.sagepub.com/supplemental.

Corresponding Author:
Coen C. Paulusma, Tytgat Institute for Liver and Intestinal Research, Academic Medical Center, S-1-168, Meibergdreef 69-71, 1105 BK Amsterdam, Netherlands.
E-mail: c.c.paulusma@amc.uva.nl

of the vesicle-generating machinery (Muthusamy et al. 2009; Paulusma and Oude Elferink 2010). In addition, studies on the (patho)physiology of ATP8B1 have indicated that P4 ATPases are, either directly or indirectly, important in maintaining an optimal physical state of the (plasma) membrane, which is essential for proper membrane barrier and membrane protein function (Paulusma et al. 2010).

P4 ATPases act in concert with members of the conserved CDC50 protein family, probable β-subunits for these proteins. The mammalian genome encodes three CDC50 proteins, CDC50A-C, which are glycosylated, ~50-kDa, two-membrane-spanning proteins (Katoh and Katoh 2004). Accumulating evidence indicates that CDC50 proteins are required for stability and exit of P4 ATPases from the endoplasmic reticulum (ER). In nonpolarized cell lines, ectopically expressed CDC50A and CDC50B facilitate exit of multiple P4 ATPases from the endoplasmic reticulum and colocalize to the plasma membrane and/or the endomembrane system (Paulusma et al. 2008; Bryde et al. 2010; van der Velden et al. 2010; Coleman and Molday 2011). Ectopic expression of CDC50A in polarized, hepatocyte-derived, WIF-B9 cells resulted in a predominant apical localization but also to subapical and endosomal vesicles when coexpressed with ATP8B1 (Paulusma et al. 2008). Apart from facilitating exit of the P4 ATPase out of the ER, it is poorly understood how mammalian CDC50 proteins contribute to the function of the P4 ATPase. Studies in the plant *Arabidopsis*, which expresses 12 P4 ATPases and 5 Cdc50 orthologs, have demonstrated that Cdc50 proteins do not determine subcellular localization nor substrate specificities of the interacting P4 ATPase; however, assembly of Cdc50 proteins with the P4 ATPase was essential for obtaining a functional heterodimer (Lopez-Marques et al. 2010). Recently, data were published to indicate an essential function of CDC50A in the reaction cycle of ATP8B1 and ATP8B2 (Bryde et al. 2010), while Coleman and Molday (2011) demonstrated phosphatidylserine flipping activity upon reconstitution of CDC50A and ATP8A2 into liposomes; furthermore, these authors showed that endogenous CDC50A and ATP8A2 are present as a heterodimer in photoreceptor disc membranes.

In the present study we analyzed murine tissue distribution and cellular localization of CDC50A with special emphasis on the liver. In liver, CDC50A is present as a complex-glycosylated protein that resides in detergent-resistant membranes in hepatocytes and sinusoidal endothelial cells. In addition, the localization of CDC50A in several tissues and cell lines was studied.

Materials and Methods

Cell Culture and Lentiviral Transduction

CHO cells (UPS-1) and WIF-B9 cells were cultured in Dulbecco's modified Eagle's medium (DMEM) (Lonza, Verviers, Belgium) supplemented with 10% fetal calf serum, 2 mM glutamine, and 0.1 U/ml penicillin/streptomycin at 37°C in a 10% C02 atmosphere. For lentiviral transduction, cells were grown to 50%–60% confluence and incubated with virus-containing supernatants/DMEM (1:1) supplemented with 10 μg/ml diethylaminoethyl-dextran for 4 hours. Lentiviral vectors containing ATP8B1, N-terminal HA-tagged CDC50A (HA-CDC50A), and HA-CDC50B complementary DNA (cDNA) have been described (Paulusma et al. 2008). Recombinant lentivirus was produced as described (Seppen et al. 2002).

Quantitative Polymerase Chain Reaction

Total RNA was extracted from homogenized mouse tissue using Trizol reagent (Invitrogen, Breda, Netherlands). cDNA was synthesized from total RNA with oligo-dT12–18 primer and Superscript III reverse transcriptase (Invitrogen). Real-time PCR measurements were performed at 60ºC in a Light Cycler 480 apparatus (Roche, Mannheim, Germany) with Light Cycler Fast start DNA Master Plus SYBR Green I (Roche). The primer sequences are as follows: Cdc50a: 5′-gaagaaatgaagacagacc-3′ and 5′-ggcaaccagatacaattctaacg-3′; Cdc50b: 5′-ccagttccgctccgacggtc-3′ and 5′-gagcgagaaggagtcgttg-3′; Cdc50c: 5′-gacaccacctctacaggaaattcag-3′ and 5′-cactgacgctgttggcctcttttgc-3′; cyclophilin: 5′-tcggagcgcaatatgaaggt-3′; and 5′-aaaaggaagacgacggagcc-3′.

Production of Polyclonal Antibodies

Polyclonal antibodies to CDC50A were raised in rabbits against synthetic peptides corresponding to the N- and C-terminus of the human protein (Double X program, Eurogentec, Seraing, Belgium). The following peptide sequences were selected: AMNYNAKDEVDGGPPC (N-terminus, residues 1–17) and CNHKYRNSSNTADITI (C-terminus, residues 347–361). A cysteine residue was coupled to the C- and N-terminus of respectively the 1–17 peptide and 347–361 peptide for coupling to MBS-(m-maleimidobenzoic acid N-hydroxysuccinimide ester) conjugated KLH (keyhole limpet hemocyanin) carrier protein. After the first immunization and 4 successive boosts, the animals were bled. Antiserum was affinity purified after coupling of the peptides to Toyopearl AF-Amino-650 media resin. In a Western blot, the C-terminal and N-terminal affinity-purified antibodies and the total serum showed the same results. In the immunostainings, the C-terminal affinity-purified antibody was applied; the N-terminal affinity-purified antibody displayed the same staining pattern.

Preparation of Cell Lysates and Western Blot Analysis

Total cell lysates were prepared from cultured cells by the scraping of cells in a hypotonic lysis buffer (10 mM

Tris-HCl, pH 7.4, 10 mM KCl, and 1.5 mM MgCl2) supplemented with Complete Protease Inhibitor Cocktail (Roche). Cells were homogenized by sonication. Protein samples were analyzed by Western blotting as described (Paulusma et al. 2008). Protein was detected with rabbit polyclonal anti-CDC50A antiserum, rat monoclonal anti-HA (Hemagglutinin antigen; clone 3F10; Roche), mouse monoclonal to glutamine synthetase (Transduction Laboratories), rabbit polyclonals to ATP1A1 (C356-M09; kindly provided by Dr. J. B. Koenderink) (Koenderink et al. 2003), ATP8B1 (Eppens et al. 2001) and caveolin (Santa Cruz Biotechnology, Santa Cruz, CA), and secondary peroxidase-conjugated immunoglobulin G. Immune complexes were visualized with Lumi-Light Western blotting substrate (Roche). Chemiluminescence was detected and quantified with a Lumi-Imager F1 and LumiAnalyst 3.1 software (Roche).

Glycosidase Treatments of CHO and Mouse Liver Cells

Parenchymal, nonparenchymal, and CHO cell lysates (50 µg protein) were treated with endoglycosidase H (Roche) and PNGase F (New England Biolabs, Ipswich, MA) according to the manufacturers' instructions. Endo H-treated lysates were first denatured in 0.02% SDS/1% β-mercaptoethanol for 10 minutes at 37ºC. Endo H and PNGase F were incubated for 2 hours at 37ºC, and samples were analyzed by Western blotting.

Immunohistochemical Analyses

Immunohistochemical analyses were performed as described previously (He et al. 2010). Briefly, tissues were fixed in 4% paraformaldehyde in phosphate-buffered saline (PBS) overnight at 4ºC, embedded in paraffin, and sectioned at 7 µm. Paraffin-embedded sections were dewaxed, rehydrated, and autoclaved for 10 min in 0.01 M sodium citrate buffer (pH 6.0) to retrieve epitopes. Endogenous peroxidase activity was blocked with 0.03% H2O2. Sections were blocked in Teng-T (10 mM Tris/HCl, pH8.0, 5 mM EDTA, 150 mM NaCl, 0.25% gelatin [w/v], 0.05% Tween-20 [v/v]) for 1 hr at room temperature (RT) and incubated with C-terminal affinity-purified CDC50A antibody, anti-glutamine synthetase, or horse radish peroxidase (HRP)–conjugated Arachis hypogaea lectin (peanut agglutinin, PNA; EY Laboratories Inc.) for 16 hr at 4°C. As secondary antibodies, HRP-conjugated goat anti-rabbit or mouse IgG (Dako, Heverlee, Belgium) were used. In the negative control, the first antibody was omitted from the incubation. HRP was visualized by incubating the slides with metal enhanced 3,3′-diaminobenzidine (DAB) substrate according to the manufacture's instructions (Pierce, Rockford, IL). Periodic acid–Schiff (PAS) staining (glycogen) was performed by incubating the sections with 0.5% periodic acid for 30 minutes. Sections were mounted in Entellan.

Indirect Immunofluorescence

CHO cells and WIF-B9 cells were grown on glass coverslips and fixed in 2% paraformaldehyde in PBS for 20 minutes at RT. After permeabilization in 0.1% Triton X-100 in PBS (PBS/Tx), cells were incubated with N-terminal affinity-purified CDC50A antibody, anti-HA (clone 3F10; Roche), anti-TGN38 (BD Transduction Laboratories), or anti-MRP2 (M2III6; Abcam) in PBS/Tx for 1 hr at RT. In the negative control, the first antibody was omitted from the incubation. The immunoreactivity was visualized with goat-anti-rat, affinity-purified, Texas Red–conjugated IgGs (Rockland) or goat-anti-mouse or goat-anti-rabbit alexa 594 (Molecular Probes), incubated in PBS/Tx for 1 hr at RT. After the first and secondary antibody incubations, coverslips were washed 5 × 5 min with PBS/Tx. Frozen mouse tissue sections were air-dried, fixed in 100% acetone for 10 min at RT, and blocked for 1 hr at RT in 5% normal goat serum in PBS/0.05% Tween-20 (PBS/Tw). All other incubations were as described above. Sections were mounted in Vectashield/DAPI (Vector Laboratories) and studied in a Leica DM-RA2 fluorescent microscope or a TCS-SP2 confocal microscope.

Isolation of Mouse Liver Cell Fractions

Mouse liver cells were isolated as described previously (Oude Elferink et al. 1989). Briefly, mouse livers were perfused in situ with 20 mg collagenase IV (Sigma). After perfusion, cells were dispersed with a coarse comb and filtered through nylon gauze. The filtrate was centrifuged 4 min at 60 × *g*. Hepatocytes and nonparenchymal cells resided in the pellet and supernatant, respectively. To purify sinusoidal endothelial cells, the nonparenchymal cell population was incubated with anti-CD146 MACS microbeads (Miltenyi Biotec, Leiden, Netherlands), according to the manufacturer's instructions; CD146-positive cells were magnetically captured by the MACS Separator. Cell fractions were analyzed by flow cytometry and Western blotting.

Isolation of Detergent-Resistant Mouse Liver Membranes

Detergent resistant membranes were extracted from mixed liver plasma membranes (mLPM). mLPMs, cLPMs, and bLPMs were isolated as described previously (Paulusma et al. 2009). mLPMs were solubilized in ice-cold 1% (v/v) Triton X-100 in PBS, mixed with an equal volume of 80% sucrose (w/v). A continuous 30%–5% sucrose (w/v) gradient was layered on top of the solubilized membranes (in

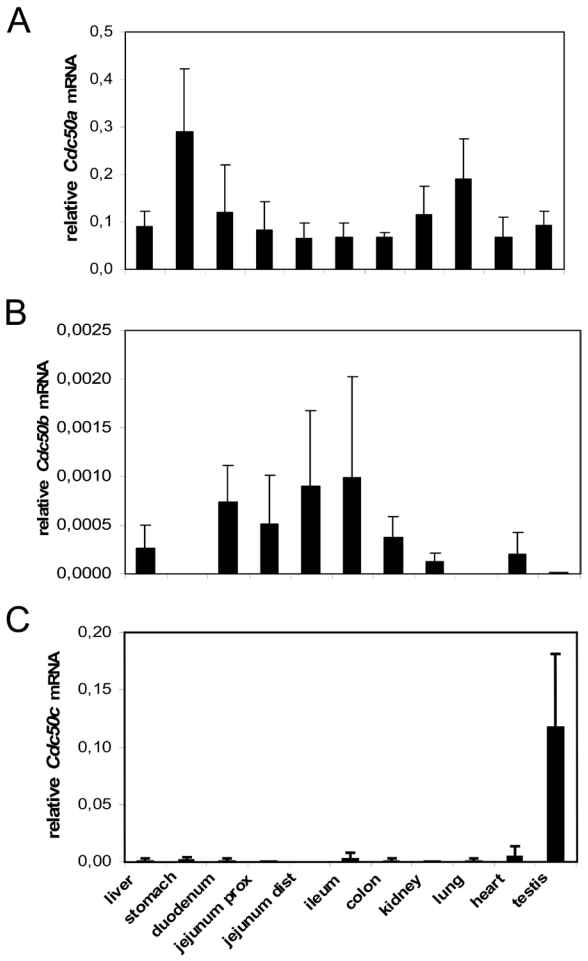

Figure 1. Expression levels of Cdc50 transcripts in mouse tissue. Real-time PCR analyses were performed on a panel of mouse tissues. The expression levels of (A) Cdc50a, (B) Cdc50b, and (C) Cdc50c were normalized for the housekeeping gene 36b4.

40% sucrose). Twelve 1-ml fractions were taken from the top of the gradient. Fractions were analyzed for alkaline phosphates activity using a Novostar analyzer (BMG Labtech GmbH, Germany) as described (Paulusma et al. 2006).

Results

Tissue Distribution of Cdc50 mRNA in Mice

Tissue distribution of the three Cdc50 homologues was assessed in a panel of mouse tissues. As shown in Fig 1, Cdc50a mRNA was expressed in similar amounts in all tissues examined. Cdc50b mRNA was more or less confined to the gastrointestinal tract, and its expression levels were approximately 100-fold lower compared to Cdc50a. Cdc50c mRNA was highly and almost exclusively expressed in the testis. These data show that Cdc50a is ubiquitously expressed and is the most prominent Cdc50 homolog in mouse tissues.

Characterization of CDC50A Antiserum

Antibodies to CDC50A were raised against synthetic peptides corresponding to the N- and C-termini of the human protein (Fig 2A). The N- and C-terminal peptides displayed respectively 82% and 100% amino acid identity with the corresponding mouse CDC50A sequences. To assess antibody specificity, we stably expressed HA-tagged human CDC50A in Chinese hamster ovary (CHO) cells. In a Western blot, the CDC50A antiserum recognized one band with an apparent molecular mass of ~50 kDa in cells expressing HA-CDC50A (Fig 2B). In control CHO cells and cells expressing HA-CDC50B, no protein bands were detected, indicating that the CDC50A antiserum specifically reacts with CDC50A. Cells were seeded on glass cover slips and stained with affinity-purified CDC50A antibody (Fig 2C). Fluorescent signal was only detected in HA-CDC50A overexpressing CHO cells, indicating that the antiserum was also suitable for immunohistochemical analyses. CDC50A expression was analyzed in several mouse tissues and in parenchymal and nonparenchymal cell fractions using C-terminal affinity-purified antibody. Several protein bands were detected of which one prominent band disappeared after using a 5-fold excess of competing peptide (Suppl Fig 1). This was, in particular, evident in liver cell fractions. Peptide competition experiments were also performed in immunofluorescent detection of CDC50A immunosignal in liver and kidney using C-terminal affinity-purified antibody. In these experiments, excess peptide resulted in complete loss of CDC50A immunostaining (Suppl Fig 2). These experiments indicate that the CDC50A antibody specifically reacted with the C-terminal CDC50A sequence.

Immunohistochemical Detection of CDC50A in Mouse Liver

CDC50A immunostaining was observed in membranes of cells lining the sinusoids (Fig 3A, D, E). Interestingly, CDC50A immunostaining was zonally distributed throughout the liver (Fig 3A); intense staining was observed in the pericentral area (demonstrated by glutamine synthetase staining of a parallel section; Fig 3C), which gradually decreased toward the periportal area. Larger magnifications (Fig 3F) revealed intracellular staining in small nuclei-containing cells. These stainings suggest that CDC50A localizes to the plasma membrane, and possibly to intracellular vesicles, of pericentral hepatocytes and/or endothelial cells lining the sinusoids.

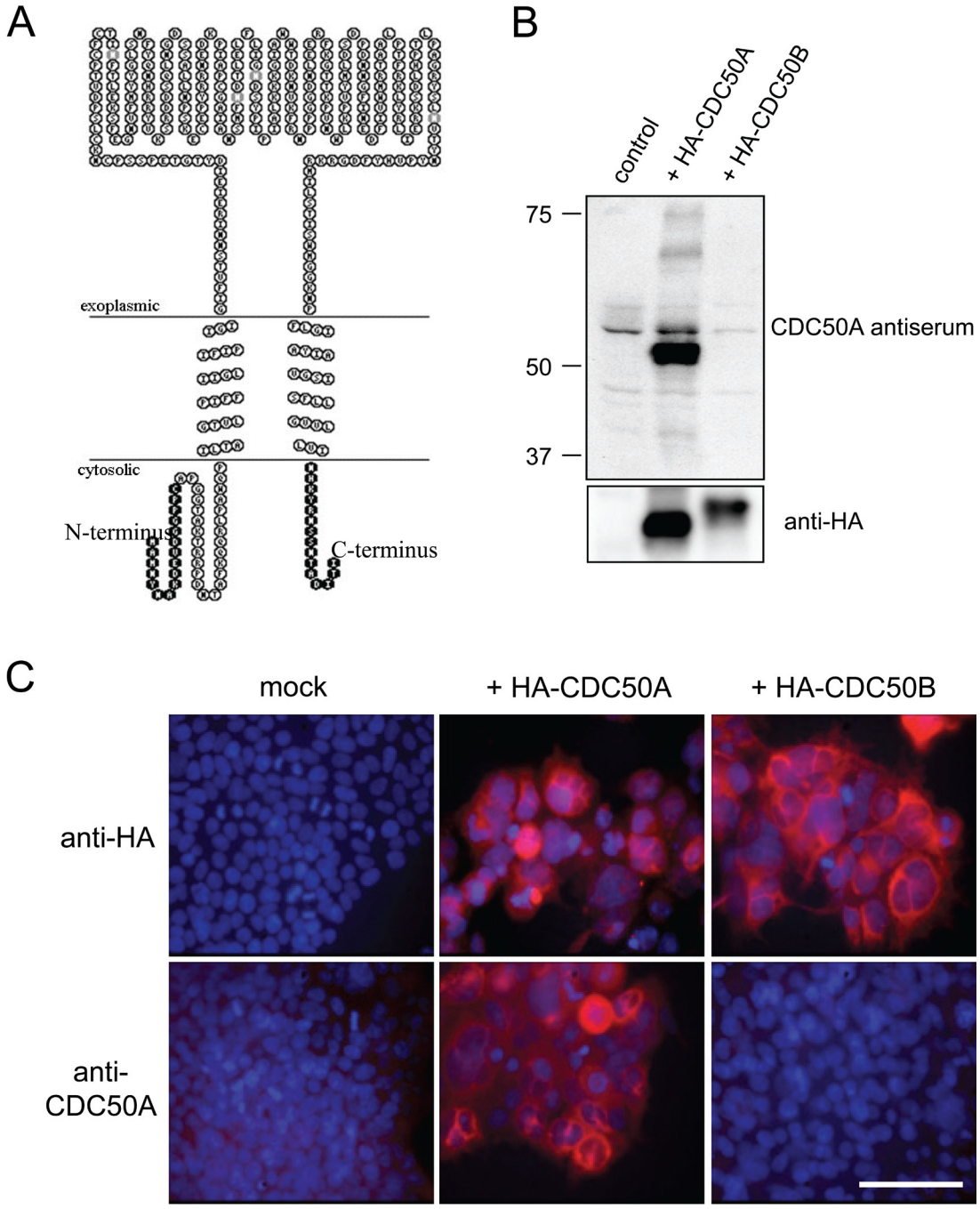

Figure 2. CDC50A antiserum specifically recognizes the CDC50A antigen. (A) CDC50A protein highlighting the N- and C-terminal amino acid stretches to which antiserum was raised (in black). TM domains determined by TMHMM Server v. 2.0 software at http://www.cbs.dtu.dk/services/TMHMM. Two-dimensional topology image created by TOP02 software at http://www.sacs.ucsf.edu/TOP02/. Four potential N-glycosylation sites are depicted in grey. The theoretical molecular weight of the protein is 40.69 kDa (including HA-tag: 41.77-kDa). CHO cells were transduced with lentiviral stocks encoding HA-CDC50A or HA-CDC50B. (B) Total cell lysates were subjected to SDS-PAGE and immunoblotting. Blots were incubated with CDC50A antiserum (upper panel) or anti-HA (lower panel). (C) Cells grown on glass cover slips were stained with N-terminal affinity-purified CDC50A antibody or anti-HA. Bar = 50 µm.

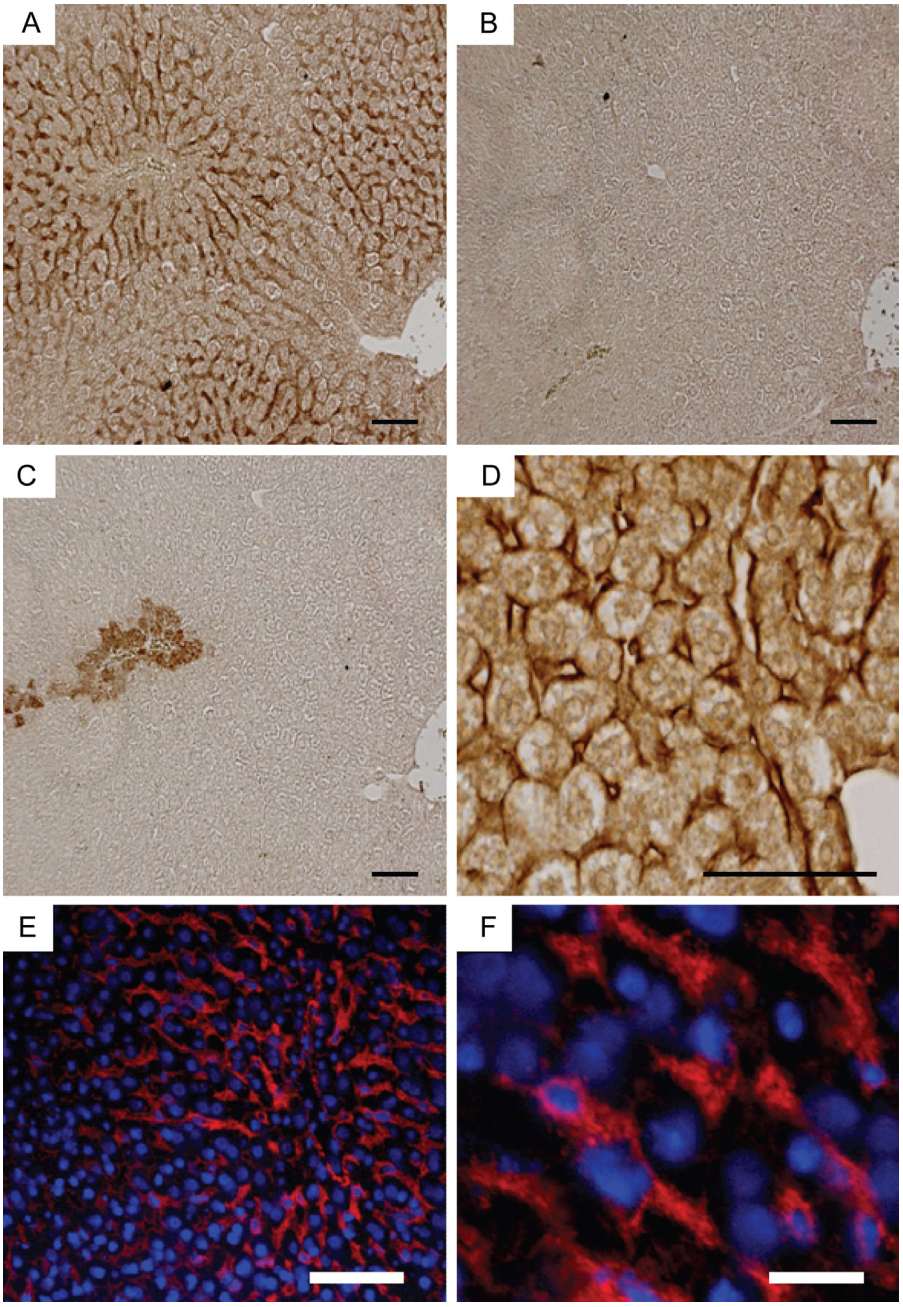

Figure 3. CDC50A immunostaining is concentrated in the pericentral areas in mouse liver and localizes intracellularly and to membranes of cells lining the sinusoids. Serial paraplast sections of mouse liver were immunohistochemically stained with C-terminal affinity-purified CDC50A antibody (A, D) or glutamine synthetase antibody (C). Negative control is displayed in panel B (A–C). (F) Confocal images highlighting intracellular CDC50A staining. Negative control in (E). Bars A–D = 50 µm, Bar E = 75 µm, Bar F = 18.18 µm.

MACS and (Detergent-Resistant) Membrane Isolations of Liver Cells

Next, we studied CDC50A-positive cell type(s) and membrane domains in mouse liver. Livers were fractionated into a parenchymal (hepatocyte-containing) and nonparenchymal cell fraction. From the nonparenchymal fraction, liver sinusoidal endothelial cells (LSEC) were isolated using CD146-MACS beads. CD146 is a membrane marker of endothelial cells (Harder et al. 1991). Purity of the cell fractions was analyzed by FACS analysis (Fig 4A) and Western blotting for the hepatocyte-specific marker glutamine synthetase. Immunoblotting revealed CDC50A in all fractions (Fig 4B). Furthermore, mixed liver plasma membranes were separated into canalicular (cLPM) and basolateral membranes (bLPM) by sucrose density centrifugation and analyzed for CDC50A expression (Fig 4C). Purity of these fractions was assessed with the basolateral resident SLC10A1 (basolateral bile salt transporter) and the canalicular resident ABCC2 (MRP2). CDC50A

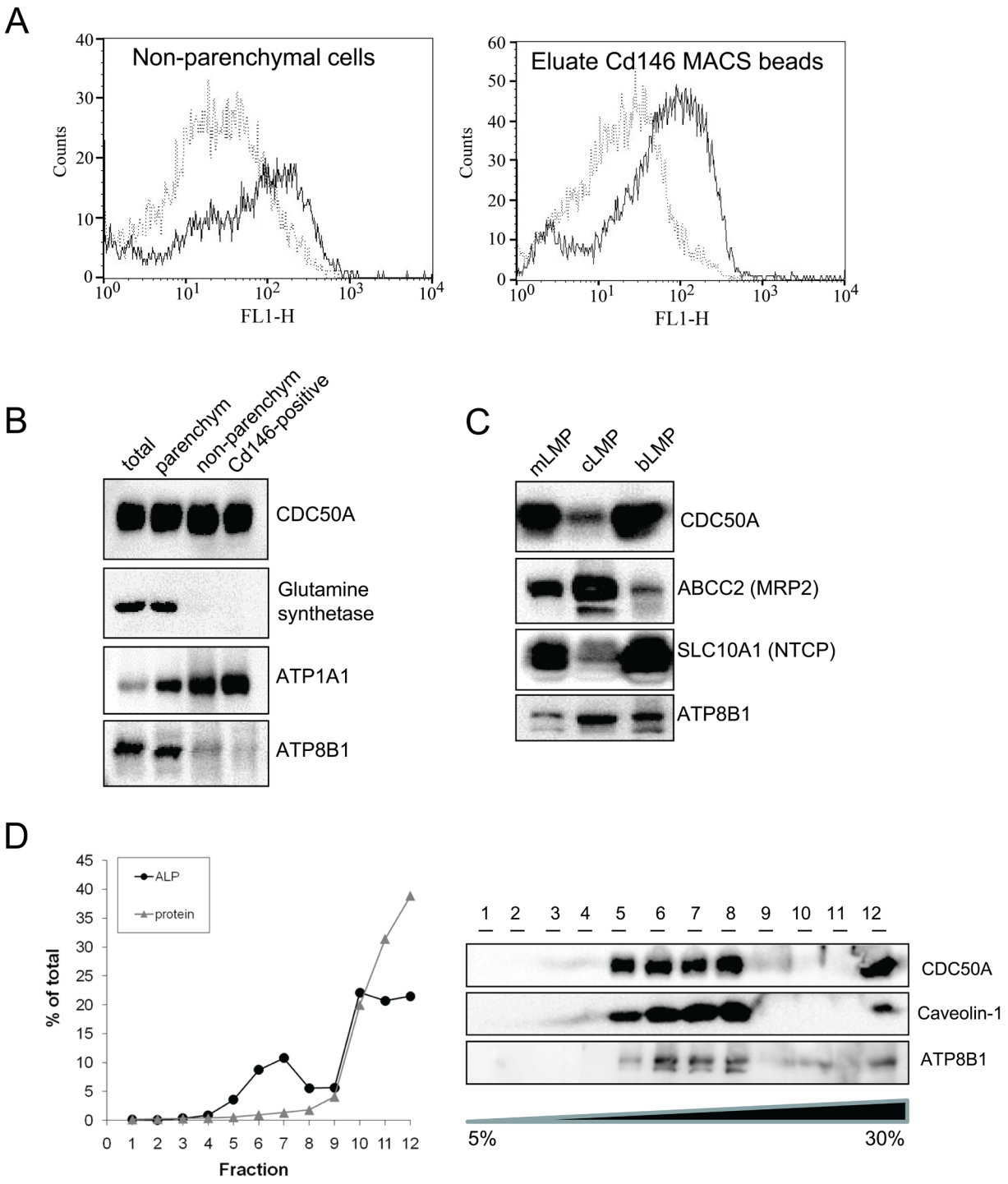

Figure 4. CDC50A is expressed in detergent-resistant membranes of hepatocytes (parenchymal) and liver sinusoidal endothelial cells. Cell fractions were isolated as described in Materials and Methods. (A) FACS scan profiles demonstrate an enrichment of CD146-positive cells in the eluate compared to the nonparenchymal cell fraction. Cells were labeled with FITC-conjugated anti-Cd146 (black curve) and a rat FITC-conjugated IgG2a K isotype control (gray curve). (B) Western analyses of cell fractions analyzed for CDC50A, glutamine synthetase, ATP1A1, and ATP8B1. (C) Western analyses of mixed (m), canalicular (c), and basolateral (b) liver plasma membranes (LPM) for CDC50A, ABCC2, SLC10A1, and ATP8B1 expression. (D) Analysis of alkaline phosphatase activity and CDC50A, caveolin-1, and ATP8B1 expression in TX-100 resistant membranes. Blots were incubated with CDC50A antiserum. Representative experiments of at least three independent experiments are shown.

predominantly resided in bLPMs, but lower levels were also observed in the canalicular fraction. These plasma membrane preparations have some contamination with ER membranes, but the detergent resistance (see below) precludes the possibility that substantial amounts of CDC50A reside in this compartment. Finally, mouse liver membranes were solubilized in 1% Triton X-100 and run on a 30% to 5% continuous sucrose gradient. CDC50A cofractionated with alkaline phosphatase activity and caveolin-1 (Fig 4C), both of which reside in detergent-resistant membrane domains. ATP8B1 was also present in CDC50A-enriched fractions. Collectively, these data indicate that CDC50A predominantly resides in detergent-resistant membranes of hepatocytes and LSECs.

Glycosidase Treatment of CDC50A

Next, we analyzed the glycosylation status of CDC50A in mouse liver cells. PNGase treatment of parenchymal and nonparenchymal cell lysates resulted in the appearance of the deglycosylated protein running at a molecular weight comparable to the theoretical molecular weight of ~40 kD (band C in Fig 5A, lanes 4, 7). Endo H treatment resulted in the appearance of one protein band with a slightly higher electrophoretic mobility, indicating that at least one of the four potential N-glycosylation sites in CDC50A is decorated with high-mannose oligosaccharides (band B in Fig 5A, lanes 3, 8). In contrast to mouse liver cells, HA-CDC50A was predominantly present as a core-glycosylated, endo H-sensitive protein upon ectopic expression in CHO cells (Fig 5B, lane 3); however, coexpression with ATP8B1 resulted in the appearance of terminally glycosylated HA-CDC50A protein (band A in Fig 5B, compare lanes 1 and 6), which upon endo H treatment displayed a similar shift in molecular weight, as was seen in mouse liver lysates (band B, compare Fig 5B, lane 8 and Fig 5A, lane 3). These data indicate that in mouse liver cells, CDC50A is present as a terminally glycosylated protein and suggest that CDC50A is present as a heterodimer with a P4 ATPase in the plasma membrane and/or membranes of endosomes and/or GA.

CDC50A Localization in Hepatic WIF-B9 Cells

Subcellular localization of endogenous CDC50A was assessed in hepatocyte-derived WIF-B9 cells. CDC50A (Fig 6A,D) did not costain with the canalicular membrane marker MRP2 (Fig 6B) but partially localized to a juxtanuclear compartment positioned between the nucleus and the canalicular membrane that costained with the trans-Golgi network (TGN; Fig 6E). We were not able to detect CDC50A staining in polarized HepG2 cells, possibly due to very low expression levels of the protein.

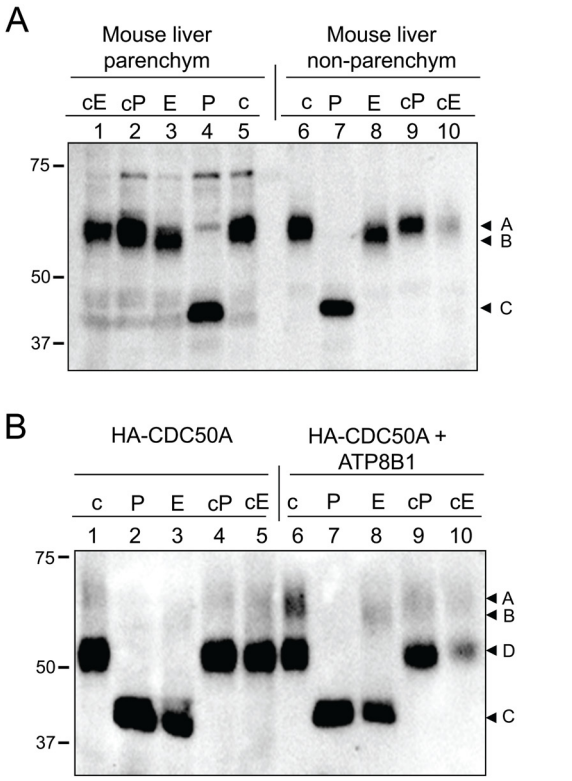

Figure 5. CDC50A is present as a terminal glycosylated protein in parenchymal and nonparenchymal cells. (A) Glycosidase treatments of liver parenchymal (lanes 1–5) or nonparenchymal fractions (lanes 6–10). (B) Glycosidase treatments of lysates of CHO cells ectopically expressing HA-CDC50A (lanes 1–5) and CHO cells coexpressing HA-CDC50A and ATP8B1 (lanes 6–10). Blots were incubated with CDC50A antiserum. A, terminal glycosylated protein; B, CDC50A band appearing after EndoH treatment; C, deglycosylated protein; D, core-glycosylated protein. c, untreated control; P, PNGase F-treated; E, Endo H-treated; cP, PNGase F control; cE, Endo H control.

Localization of CDC50A in Other Tissues of the Mouse

In the pancreas, strong CDC50A immunostaining was observed in zymogen granules, secretory vesicles containing digestive enzymes that are present in the acinar cells of the exocrine pancreas (Fig 7). In addition, CDC50A staining was observed in the islets of Langerhans (Fig 8). The CDC50A-positive cells most probably reflect the insulin producing and secreting β-cells, because of their predominance and central core location in the islet. In the stomach, anti-CDC50A stained the gastric chief cells in the base of the gastric glands (Fig 9). Chief cells synthesize many digestive enzymes, which are stored in secretory vesicles. Similar to the pancreatic acinar cell, CDC50A staining was also granular and concentrated in the apical region near the glandular lumen where the enzymes are excreted.

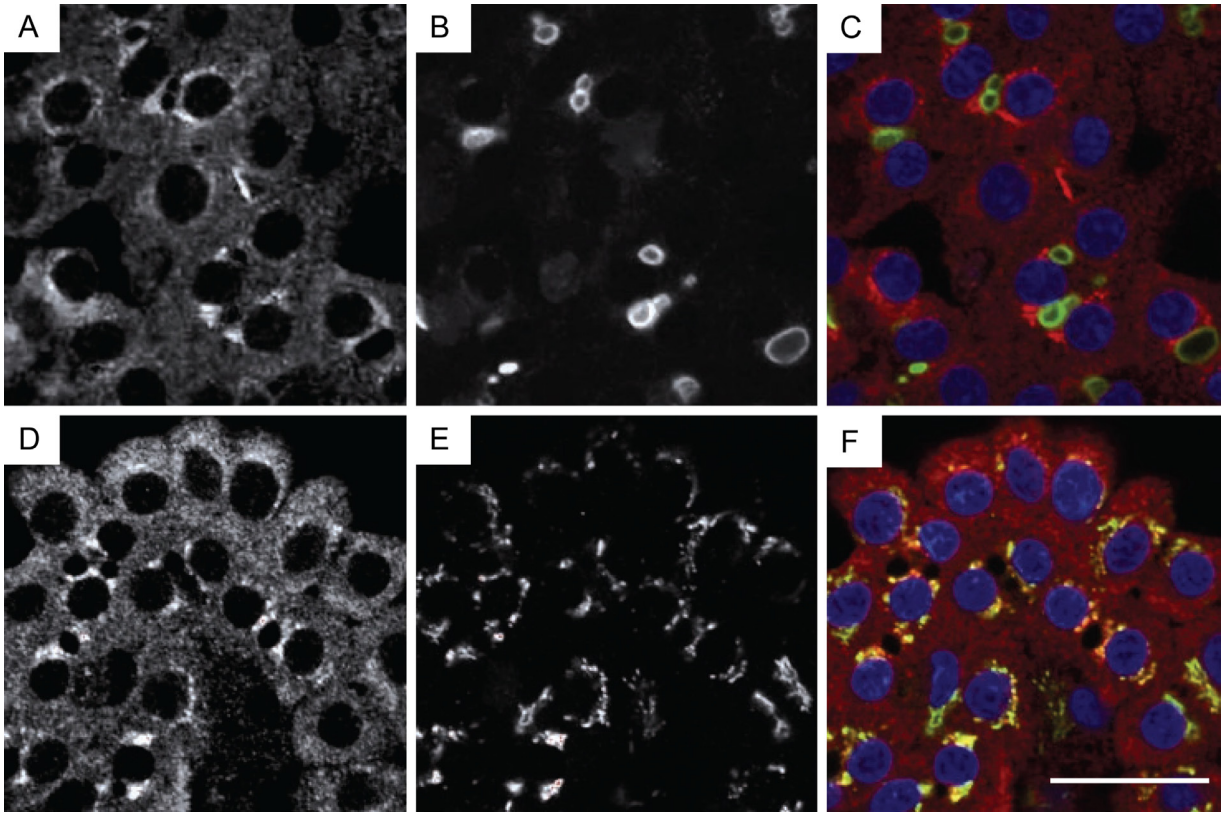

Figure 6. CDC50A partially costains with the trans-Golgi network in polarized WIF-B9 cells. WIF-B9 cells were costained for CDC50A (A) and MRP2 (B) or CDC50A (D) and TGN38 (E); (D) and (F) are merged pictures (red, CDC50; green, MRP2 or TGN38; blue, nuclear DAPI staining); N-terminal affinity-purified CDC50A antibody was used. Bar = 50 µm.

Figure 10A shows staining of CDC50A in tubules in the renal cortex, whereas the renal medulla is negative for CDC50A. CDC50A immunosignal was detected at the apical border of the cells lining PAS-positive, proximal convoluted tubules (Fig 10B,E) and in the medullary ray in the outer medulla (Fig 10C).

Discussion

In mammals, 3 CDC50 proteins and 14 P4 ATPases (15 in mice) are expressed (Paulusma and Oude Elferink 2010). Accumulating in vitro evidence suggests that CDC50 proteins are the β-subunits of P4 ATPases, which can form a functional lipid-flipping protein heterodimer (Paulusma et al. 2008; Bryde et al. 2010; Coleman and Molday 2011). Recently, CDC50A and ATP8A2 were copurified from photoreceptor membranes and displayed phosphatidylserine flipping activity upon reconstitution into liposomes (Coleman and Molday 2011). Most likely, many, if not all, P4 ATPases interact with a CDC50 protein; however, the specificity of physiological relevant CDC50–P4 ATPase interactions is presently not known.

Cdc50a is the most abundant and ubiquitously expressed Cdc50 isoform in mice. In mouse liver, CDC50A localized to liver sinusoidal endothelial cells (LSECs) and to the plasma membrane (mostly basolateral) of hepatocytes. Interestingly, CDC50A is zonally distributed with highest expression in the pericentral areas. Despite morphological uniformity of hepatocytes, many metabolic pathways in the liver are zonally regulated (Moorman et al. 1988; Jungermann and Kietzmann 1996); For instance, metabolism of xenobiotics by cytochrome P450 enzymes, nitrogen metabolism, and glucose uptake/storage are handled by the pericentral hepatocytes, whereas periportal hepatocytes are important for gluconeogenesis, ammonia metabolism, cholesterol synthesis, and bile formation. Furthermore, albumine mRNA expression displays a zonal expression pattern with decreasing expression going from portal to central (Moorman et al. 1990). Zonal heterogeneity of liver sinusoidal endothelial cells has been reported with regard to their filtering capacity (fenestration) and binding capacity for lectins and immune cells (Jungermann and Kietzmann 1996). Endothelial cells in the pericentral area have more but smaller fenestrae compared to periportally

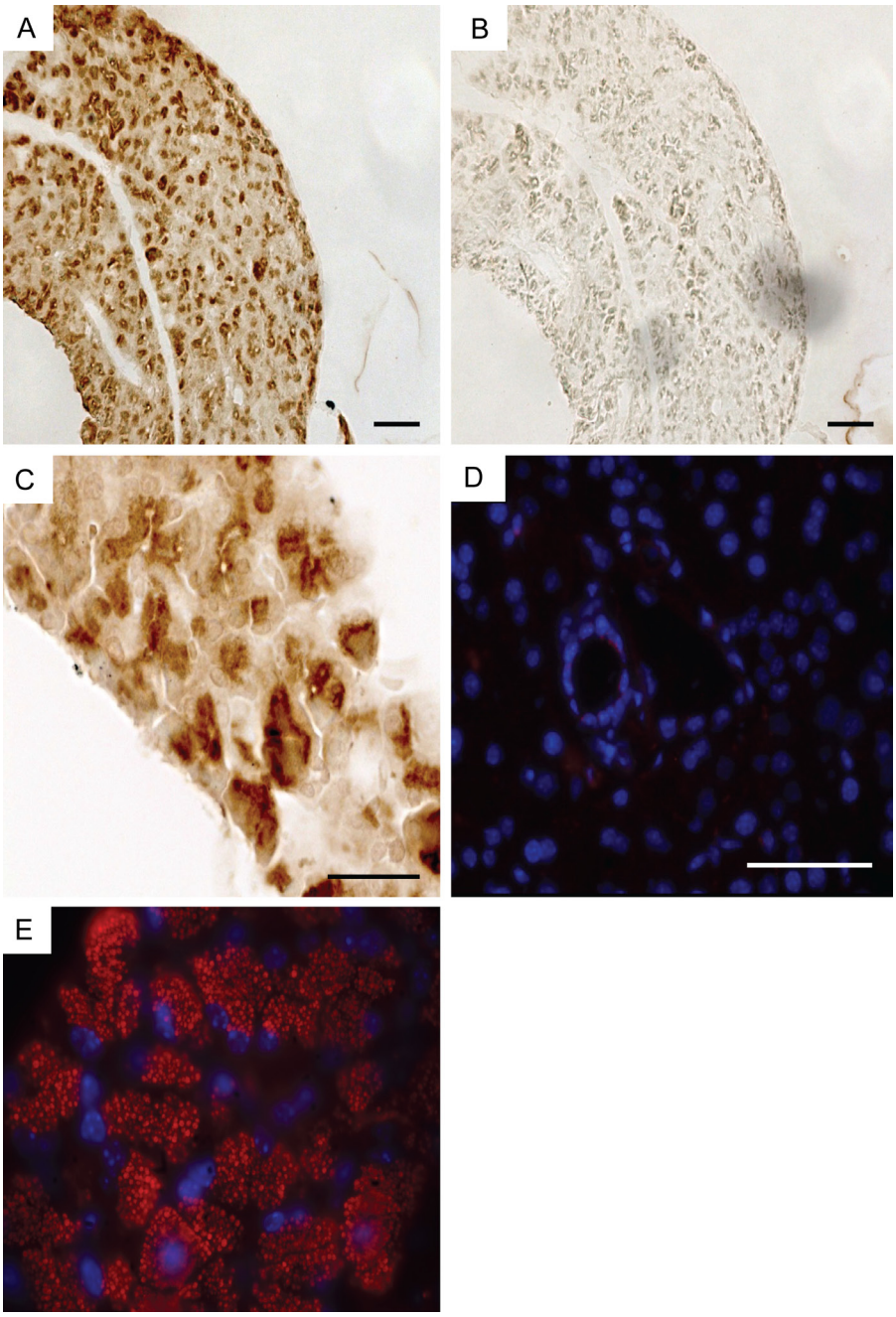

Figure 7. CDC50A is expressed in pancreatic zymogen granules in the acinar cells of the exocrine pancreas. Serial paraplast sections of mouse pancreas immunohistochemically stained with C-terminal affinity-purified CDC50A antibody (A and C). Negative control in (B). (E) Immunofluorescent detection of CDC50A and its negative control (D). Bar = 50 µm.

localized endothelial cells, resulting in a higher porosity of pericentral sinusoids. Apart from a filtering function, endothelial cells have very high endocytic activity. Since the CDC50-P4 ATPase heteromeric complexes have been implicated in vesicle biogenesis (Muthusamy et al. 2009; Paulusma and Oude Elferink 2010), it is tempting to speculate that CDC50A plays a role in endocytosis in LSECs and/or basolateral membranes of hepatocytes.

On the basis of our previous work, we hypothesized that CDC50A is the β-subunit for ATP8B1 in hepatocytes (Paulusma et al. 2008). ATP8B1 is expressed in the canalicular membrane of hepatocytes (Eppens et al. 2001; Ujhazy et al. 2001). Furthermore, ectopically expressed CDC50A and ATP8B1 colocalized in the subapical region and in the apical membrane of hepatic WIF-B9 cells (Paulusma et al. 2008). In the present study however, we

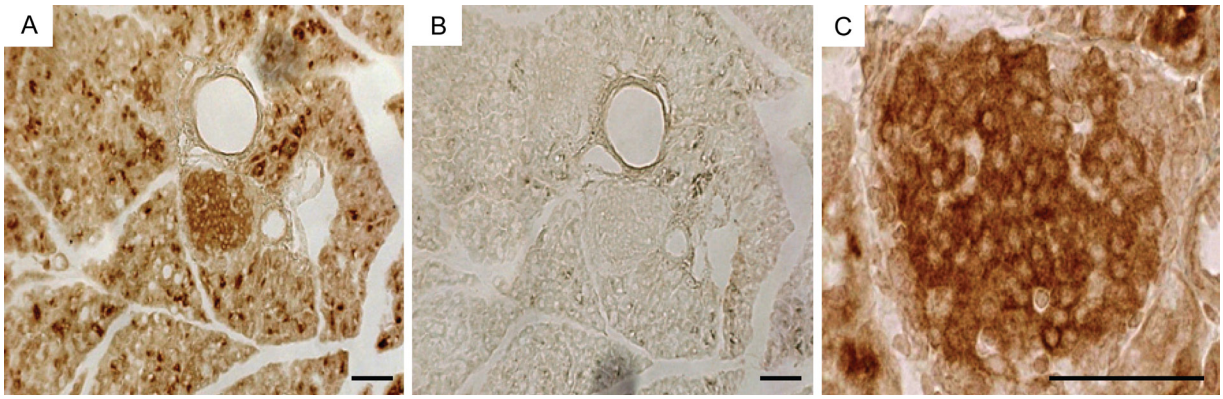

Figure 8. CDC50A is expressed in the islets of Langerhans. Serial paraplast sections of mouse pancreas immunohistochemically stained with C-terminal affinity-purified CDC50A antibody (A, C); negative control in (B). Bar is 50 µm.

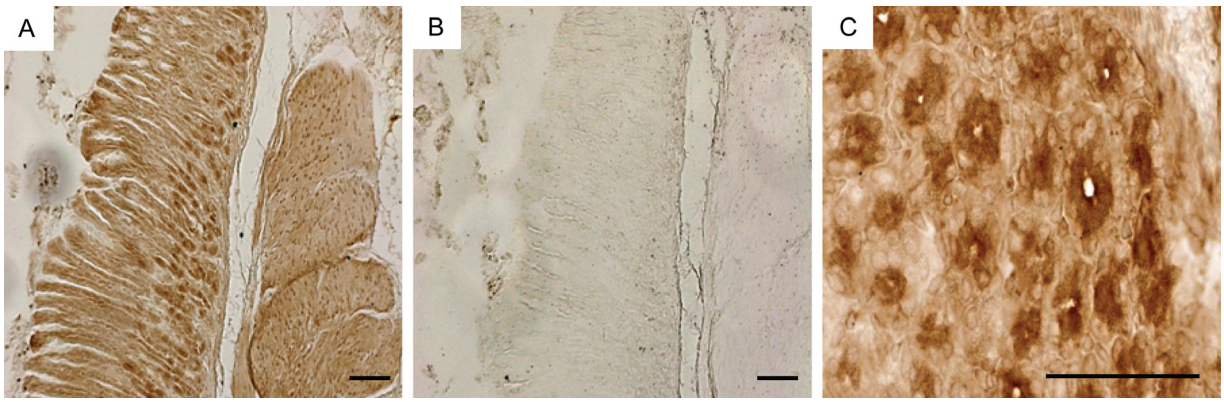

Figure 9. CDC50A is expressed in gastric zymogen granules of chief cells in the stomach. Serial paraplast sections of mouse stomach immunohistochemically stained with C-terminal affinity-purified CDC50A antibody (A and C), or negative control (B). Bar is 50 µm.

could not detect CDC50A in the canalicular membrane of mouse hepatocytes. There are several explanations for this unexpected result. First, CDC50A is not expressed, or its expression is extremely low in the canalicular membrane and is not uncovered due to high expression levels in LSECs and basolateral membranes of hepatocytes. Second, CDC50A merely functions as a chaperone and cycles between the canalicular membrane and the endomembrane system, delivering ATP8B1 to the canalicular membrane. Our deglycosylation experiments indicate that CDC50A is present as a terminal-glycosylated protein, suggesting that CDC50A is present as a late Golgi, endosomal, and/or plasma membrane-associated protein. However, the exact subcellular location of CDC50A can only be determined by using immunoelectron microscopy. Third, since ATP8B1 can assemble with both CDC50A and CDC50B in vitro (Paulusma et al. 2008; Bryde et al. 2010; van der Velden et al. 2010), it cannot be excluded that CDC50B is the physiological relevant binding partner for ATP8B1 in hepatocytes. Indeed, mouse hepatocytes do express very low levels of Cdc50b mRNA (DF, unpublished results).

It thus remains to be determined whether CDC50A and ATP8B1 form a physiological relevant protein complex in hepatocytes. It is possible that CDC50A assembles with multiple other hepatic P4 ATPases. Recently, ATP11C was identified as an important determinant of proper bile formation (Siggs et al. 2011a; Siggs et al. 2011b; Yabas et al. 2011). ATP11C is highly expressed in hepatocytes and LSECs and thus may form a heterodimer with CDC50A in both cell types. Furthermore, Coleman and Molday recently demonstrated that CDC50A and ATP8A2 exist as a heterodimer in photoreceptor membranes in the eye (Coleman and Molday 2011).

In pancreas and stomach CDC50A staining was observed in zymogen granules, which, upon stimulation, fuse with the apical membrane to release their contents. The presence of CDC50A in zymogen granules of acinar cells in the exocrine pancreas is in accordance with a proteomic analysis of

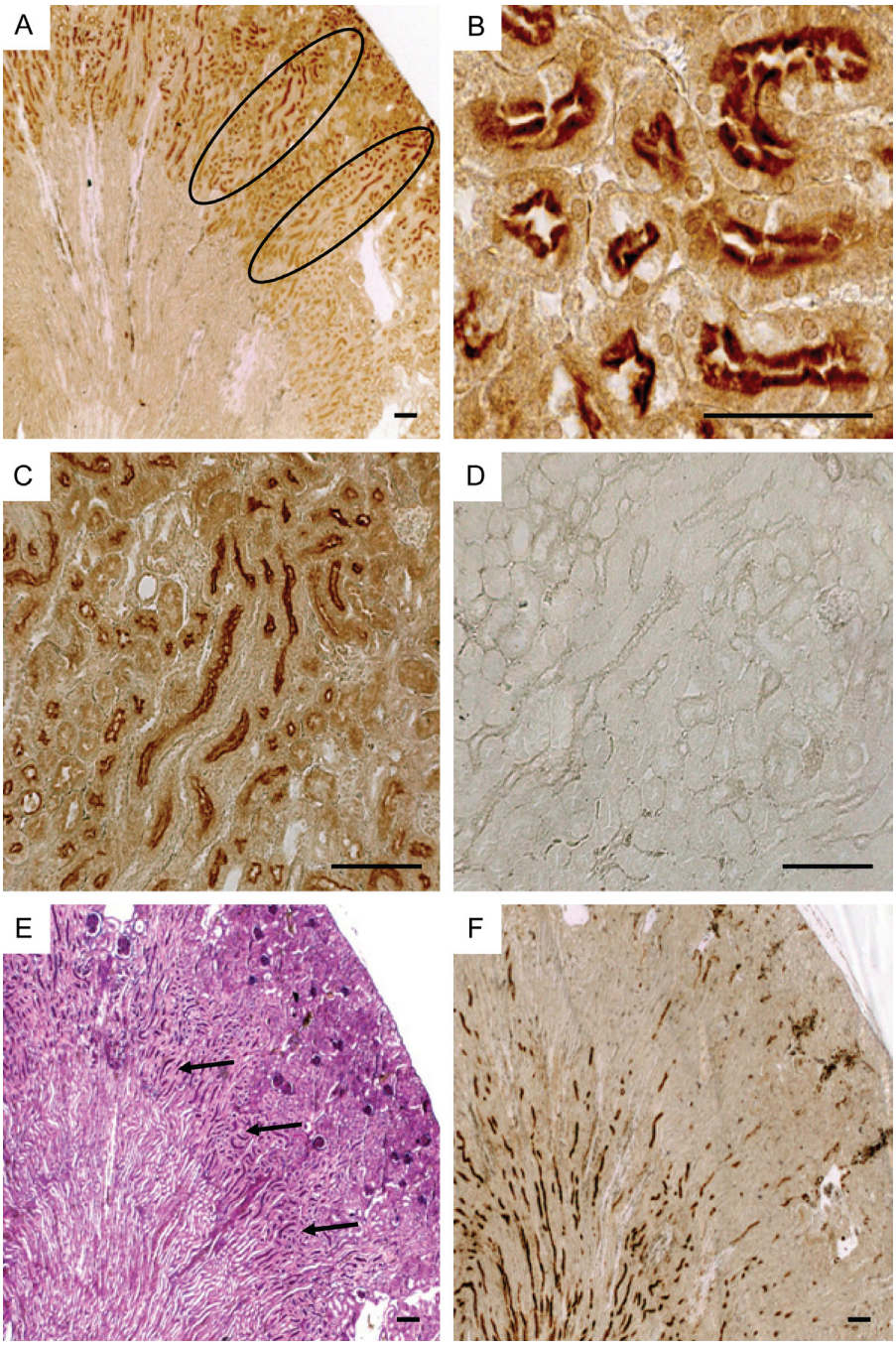

Figure 10. CDC50A localizes to the apical border of epithelial cells of the proximal convoluted tubules in the renal cortex. Serial paraplast sections of mouse kidney were immunohistochemically stained with C-terminal affinity-purified CDC50A antibody (A-C); ovals indicate the medullary rays in the cortex. Negative control in (D). (E) PAS staining to indicate the proximal convoluted tubules (arrows); (F) peanut agglutinin staining to indicate the collecting ducts in the renal medulla. Bar = 50 µm.

rat pancreatic zymogen granules, which listed CDC50A (referred to as transmembrane protein 30A) as a granular protein (Rindler et al. 2007); in addition to CDC50A, ATP8B1 and ATP8A1 were characterized as granular proteins. CDC50A staining was also observed in the insulin-secreting β-cells in the islets of Langerhans of the pancreas. As was shown in other organisms (Muthusamy et al. 2009; Paulusma and Oude Elferink 2010), our observations suggest that mammalian CDC50A (together with a P4 ATPase) may be involved in the biogenesis of transport vesicles at the TGN and/or plasma membrane. Thus, in the exocrine pancreas and stomach, CDC50A may be important in the generation of digestive enzyme-containing secretory vesicles. In the β-cells of the islands of Langerhans, CDC50A

may be important in generating insulin/amylin-containing secretory vesicles. Alternatively, CDC50A is important in generating or maintaining a fusion-competent vesicular membrane, which is a prerequisite for releasing the vesicular contents. In the kidney, CDC50A localizes to the brush border of the proximal tubules, which key function is the reabsorption of water and electrolytes (i.e., $Na+$,Cl^-, $SO4^{2-}$, and HCO_{3-}) (Markovich and Aronson 2007). CDC50A could be important in maintaining the asymmetric distribution of phospholipids within the brush border membrane, guaranteeing proper membrane protein function. Alternatively, CDC50A is an important determinant of protein trafficking to or from the brush border membrane. Whether CDC50A fulfills such functions in these mammalian cells/tissues, and if defects in this machinery lead to disease, is a subject for future research.

Acknowledgments

We wish to thank Prof. W. H. Lamers for helpful discussions and J. L. M. Vermeulen, C. Kunne, and A. Sokolović for technical assistance.

Declaration of Conflicting Interests

The authors declared no potential conflicts of interest with respect to the research, authorship, and/or publication of this article.

Funding

The authors received no financial support for the research, authorship, and/or publication of this article.

References

Bryde S, Hennrich H, Verhulst PM, Devaux PF, Lenoir G, Holthuis JC. 2010. CDC50 proteins are critical components of the human class-1 P4-ATPase transport machinery. J Biol Chem. 285:40562–40572.

Coleman JA, Molday RS. 2011. Critical role of the {beta}-subunit CDC50A in the stable expression, assembly, subcellular localization, and lipid transport activity of the P4-ATPase ATP8A2. J Biol Chem. 286:17205–17216.

Eppens EF, van Mil SW, de Vree JM, Mok KS, Juijn JA, Oude Elferink RPJ, Berger R, Houwen RH, Klomp LW. 2001. FIC1, the protein affected in two forms of hereditary cholestasis, is localized in the cholangiocyte and the canalicular membrane of the hepatocyte. J Hepatol. 35:436–443.

Folmer DE, Oude Elferink RPJ, Paulusma CC. 2009. P4 ATPases: lipid flippases and their role in disease. Biochim Biophys Acta. 1791:628–635.

Halleck MS, Lawler JF Jr., Blackshaw S, Gao L, Nagarajan P, Hacker C, Pyle S, Newman JT, Nakanishi Y, Ando H, et al. 1999. Differential expression of putative transbilayer amphipath transporters. Physiol Genomics. 1:139–150.

Harder R, Uhlig H, Kashan A, Schutt B, Duijvestijn A, Butcher EC, Thiele HG, Hamann A. 1991. Dissection of murine lymphocyte-endothelial cell interaction mechanisms by SV-40-transformed mouse endothelial cell lines: novel mechanisms mediating basal binding, and alpha 4-integrin-dependent cytokine-induced adhesion. Exp Cell Res. 197:259–267.

He Y, Hakvoort TB, Vermeulen JL, Labruyère WT, de Waart DR, van der Hel WS, Ruijter JM, Uylings HB, Lamers WH. 2010. Glutamine synthetase deficiency in murine astrocytes results in neonatal death. Glia. 58:741–754.

Holthuis JC, Levine TP. 2005. Lipid traffic: floppy drives and a superhighway. Nat Rev Mol Cell Biol. 6:209–220.

Jungermann K, Kietzmann T. 1996. Zonation of parenchymal and nonparenchymal metabolism in liver. Annu Rev Nutr. 16:179–203.

Katoh Y, Katoh M. 2004. Identification and characterization of CDC50A, CDC50B and CDC50C genes in silico. Oncol Rep. 12:939–943.

Koenderink JB, Geibel S, Grabsch E, De Pont JJ, Bamberg E, Friedrich T. 2003. Electrophysiological analysis of the mutated Na,K-ATPase cation binding pocket. J Biol Chem. 278:51213–51222.

Lopez-Marques RL, Poulsen LR, Hanisch S, Meffert K, Buch-Pedersen MJ, Jakobsen MK, Pomorski TG, Palmgren MG. 2010. Intracellular targeting signals and lipid specificity determinants of the ALA/ALIS P4-ATPase complex reside in the catalytic ALA {alpha}-subunit. Mol Biol Cell. 21:791–801.

Markovich D, Aronson PS. 2007. Specificity and regulation of renal sulfate transporters. Annu Rev Physiol. 69:361–375.

Moorman AF, de Boer PA, Geerts WJ, van den Zande L, Lamers WH, Charles R. 1988. Complementary distribution of carbamoylphosphate synthetase (ammonia) and glutamine synthetase in rat liver acinus is regulated at a pretranslational level. J Histochem Cytochem. 36:751–755.

Moorman AFM, de Boer PAJ, Evans D, Charles R, Lamers WH. 1990. Expression patterns of mRNAs for alpha-fetoprotein and albumin in the developing rat: the ontogenesis of hepatocyte heterogeneity. Histochem J. 22:653–660.

Muthusamy BP, Natarajan P, Zhou X, Graham TR. 2009. Linking phospholipid flippases to vesicle-mediated protein transport. Biochim Biophys Acta. 1791:612–619.

Oude Elferink RPJ, Ottenhoff R, Liefting W, de Haan J, Jansen PLM. 1989. Hepatobiliary transport of glutathione and glutathione conjugate in rats with hereditary hyperbilirubinemia. J Clin Invest. 84:476–483.

Paulusma CC, de Waart DR, Kunne C, Mok KS, Oude Elferink RPJ. 2009. Activity of the bile salt export pump (ABCB11) is critically dependent on canalicular membrane cholesterol content. J Biol Chem. 284:9947–9954.

Paulusma CC, Folmer DE, Ho-Mok KS, de Waart DR, Hilarius PM, Verhoeven AJ, Oude Elferink RPJ. 2008. ATP8B1 requires an accessory protein for endoplasmic reticulum exit and plasma membrane lipid flippase activity. Hepatology. 47:268–278.

Paulusma CC, Groen A, Kunne C, Ho-Mok KS, Spijkerboer AL, de Waart DR, Hoek FJ, Vreeling H, Hoeben KA, van Marle

J, et al. 2006. Atp8b1 deficiency in mice reduces resistance of the canalicular membrane to hydrophobic bile salts and impairs bile salt transport. Hepatology. 44:195–204.

Paulusma CC, Oude Elferink RPJ. 2005. The type 4 subfamily of P-type ATPases, putative aminophospholipid translocases with a role in human disease. Biochim Biophys Acta. 1741:11–24.

Paulusma CC, Oude Elferink RPJ. 2010. P4 ATPases: the physiological relevance of lipid flipping transporters. FEBS Lett. 584:2708–2716.

Paulusma CC, Oude Elferink RPJ, Jansen PLM. 2010. Progressive familial intrahepatic cholestasis type 1. Semin Liver Dis. 30:117–124.

Rindler MJ, Xu CF, Gumper I, Smith NN, Neubert TA. 2007. Proteomic analysis of pancreatic zymogen granules: identification of new granule proteins. J Proteome Res. 6:2978–2992.

Seppen J, Rijnberg M, Cooreman MP, Oude Elferink RPJ. 2002. Lentiviral vectors for efficient transduction of isolated primary quiescent hepatocytes. J Hepatol. 36:459–465.

Siggs OM, Arnold CN, Huber C, Pirie E, Xia Y, Lin P, Nemazee D, Beutler B. 2011a. The P4-type ATPase ATP11C is essential for B lymphopoiesis in adult bone marrow. Nat Immunol. 12:434–440.

Siggs OM, Schnabl B, Webb B, Beutler B. 2011b. X-linked cholestasis in mouse due to mutations of the P4-ATPase ATP11C. Proc Natl Acad Sci U S A. 108:7890–7895.

Ujhazy P, Ortiz D, Misra S, Li S, Moseley J, Jones H, Arias IM. 2001. Familial intrahepatic cholestasis 1: studies of localization and function. Hepatology. 34:768–775.

van der Velden LM, Wichers CG, van Breevoort AE, Coleman JA, Molday RS, Berger R, Klomp LW, van de Graaf SF. 2010. Heteromeric interactions required for abundance and subcellular localization of human CDC50 proteins and class 1 P4 ATPases. J Biol Chem. 285:40088–40096.

van der Woerd WL, van Mil SW, Stapelbroek JM, Klomp LW, van de Graaf SF, Houwen RH. 2010. Familial cholestasis: progressive familial intrahepatic cholestasis, benign recurrent intrahepatic cholestasis and intrahepatic cholestasis of pregnancy. Best Pract Res Clin Gastroenterol. 24:541–553.

Wang L, Beserra C, Garbers DL. 2004. A novel aminophospholipid transporter exclusively expressed in spermatozoa is required for membrane lipid asymmetry and normal fertilization. Dev Biol. 267:203–215.

Yabas M, The CE, Frankenreiter S, Lal D, Roots CM, Whittle B, Andrews DT, Zhang Y, Teoh NC, Sprent J, et al.. 2011. ATP11C is critical for the internalization of phosphatidylserine and differentiation of B lymphocytes. Nat Immunol. 12:441–449.